OUTSTANDING MEETING PAPERS

Review

Electronically stimulated degradation of silicon solar cells

J. Schmidt[a] and K. Bothe
Institut für Solarenergieforschung Hameln/Emmerthal (ISFH), D-31860 Emmerthal, Germany

D. Macdonald
Department of Engineering, Australian National University, Canberra ACT 0200, Australia

J. Adey, R. Jones, and D.W. Palmer
School of Physics, University of Exeter, Exeter EX4 4QL, United Kingdom

Carrier lifetime degradation in crystalline silicon solar cells under illumination with white light is a frequently observed phenomenon. Two main causes of such degradation effects have been identified in the past, both of them being electronically driven and both related to the most common acceptor element, boron, in silicon: (i) the dissociation of iron-boron pairs and (ii) the formation of recombination-active boron-oxygen complexes. While the first mechanism is particularly relevant in metal-contaminated solar-grade multicrystalline silicon materials, the latter process is important in monocrystalline Czochralski-grown silicon, rich in oxygen. This paper starts with a short review of the characteristic features of the two processes. We then briefly address the effect of iron-boron dissociation on solar cell parameters. Regarding the boron-oxygen-related degradation, the current status of the physical understanding of the defect formation process and the defect structure are presented. Finally, we discuss different strategies for effectively avoiding the degradation.

I. INTRODUCTION

Two main causes have been identified for the illumination-induced degradation of solar cells fabricated on boron-doped mono- and multicrystalline silicon materials. Both of them are electronically driven defect reactions involving substitutional boron (B_s), leading to a pronounced decrease in the carrier recombination lifetime under solar cell operating conditions. In multicrystalline silicon (mc-Si), dissociation of interstitial iron-substitutional boron (Fe_iB_s) pairs into isolated Fe_i and B_s has been identified as the most relevant process.[1] This well-known process is linked to the degree of iron contamination in the material. It can also be observed in single-crystalline iron-contaminated B-doped float-zone (FZ) and Czochralski (Cz) silicon and is not restricted to mc-Si. Another carrier lifetime degradation effect has been observed in metal-impurity-free B-doped Cz-Si.[2] This effect has only recently been attributed to the simultaneous presence of B_s and interstitial oxygen (O_i).[3,4] Interestingly, as for the Fe_iB_s dissociation, this degradation effect occurs also in the dark when minority-carriers are injected (e.g., by a forward-biased *pn* junction), leading to the conclusion that the degradation is caused by the presence of minority-carriers and photons are not directly involved.[5] However, in contrast to the Fe_iB_s-related lifetime degradation, which also occurs during annealing above ~100 °C, the latter degradation effect is fully reversible by annealing above ~200 °C; i.e., the degraded lifetime recovers during low-temperature annealing, making it relatively easy to distinguish between the two effects. Recently, much research has been devoted to the light-induced B_s–O_i-related degradation problem, which is presently the main obstacle for making Cz–Si an ideal cost-saving material for high-efficiency solar cells. This paper reviews the present physical understanding of the degradation effects and discusses different approaches for reducing or even completely avoiding them.

© 2006 Materials Research Society

II. IRON-BORON-RELATED DEGRADATION

In boron-doped p-type silicon, Fe_i is well known to form pairs with B_s.[6] These Fe_iB_s pairs dissociate into Fe_i and B_s under illumination due to a recombination-enhanced dissociation process.[7] If the silicon sample is kept in the dark at room temperature, the Fe_iB_s pairs re-form within a couple of hours for typical resistivities of around 1 Ωcm. Due to this characteristic behavior, the carrier lifetime in iron-contaminated boron-doped silicon is determined by Fe_iB_s pairs, isolated Fe_i, or a combination of both species, depending on the history of the sample. The injection level dependence of the carrier lifetimes is much more pronounced for isolated Fe_i than for Fe_iB_s pairs, and the corresponding injection-dependent lifetime curves show a characteristic cross-over point at an approximately fixed excess-carrier concentration for sufficiently low doping concentrations ($N_{dop} \ll 1.5 \times 10^{17}$ cm^{-3}).[1] Using literature data of the energy levels and capture cross sections for Fe_iB_s and Fe_i,[1,6] the crossover point can be calculated to be at $\Delta n_{cr} = 1.4 \times 10^{14}$ cm^{-3}.[1] Figure 1 shows injection-dependent lifetime curves of an iron-implanted silicon sample before and after optical dissociation of Fe_iB_s pairs, measured using the quasi-steady-state photoconductance technique (QSSPC). To distribute the implanted Fe_i homogeneously throughout the wafer, the sample has been annealed at 900 °C for 1 h. From the measurements shown in Fig. 1, we are able to determine the crossover point to be at $\Delta n_{cr} = 2 \times 10^{14}$ cm^{-3} in good agreement with the calculated value. Comparable experimental results have been reported for silicon of various resistivities using different measurement techniques.[1]

The effect of the pronounced change in the lifetime caused by the dissociation of Fe_iB_s pairs on the solar cell parameters has been studied by means of numerical device simulations using reported recombination parameters for Fe_i and Fe_iB_s.[8,9] Figure 2 shows the relative changes in the short-circuit current density J_{sc} and the open-circuit voltage V_{oc} of a high-efficiency solar cell for different total iron concentrations. Interestingly, we find that while J_{sc} always decreases as a consequence of the Fe_iB_s dissociation, V_{oc} shows a pronounced increase of up to 5% at relatively high iron concentrations. However, as the degradation in J_{sc} dominates, the cell efficiency always decreases. The very different behavior of V_{oc} and J_{sc} is due to the much larger injection level in the base of the cell under open-circuit than under short-circuit conditions. While under one-sun short-circuit conditions the excess-carrier concentration Δn within the base is always below the crossover point Δn_{cr}, the situation is different under open-circuit conditions. In the latter case, it depends on the absolute value of the carrier lifetime whether the injection level is above or below the crossover point. Hence, at high iron levels, corresponding to low lifetimes and low injection levels, V_{oc} degrades, whereas at moderate iron contamination levels, corresponding to higher lifetimes and higher injection levels, V_{oc} increases during illumination. The threshold iron contamination level of the V_{oc}-degradation was found to be about one to two orders of magnitude larger than the threshold iron levels of all other cell parameters. Hence, up to relatively high iron concentrations (typically ~10^{12} cm^{-3} for doping concentrations around 10^{16} cm^{-3}) degradation only in short-circuit current, fill factor, and efficiency may be observed, whereas the open-circuit voltage remains constant or even increases. This effect is characteristic of the Fe_iB_s dissociation and may therefore be used as a simple way of identifying iron contamination problems in silicon solar cells.

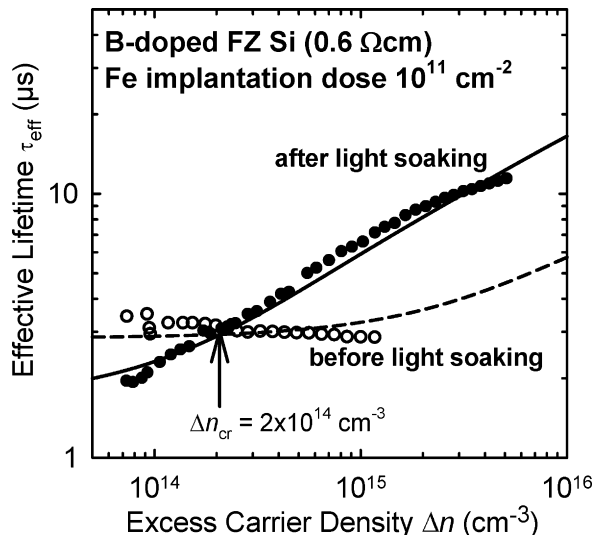FIG. 1. Injection-dependent lifetime curves of an Fe-implanted B-doped silicon wafer before an after optical dissociation of Fe_iB_s pairs, showing the characteristic crossover point Δn_{cr}.
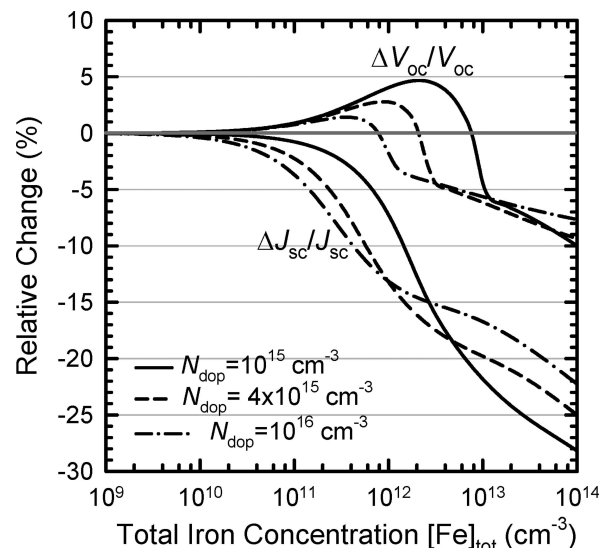

FIG. 2. Calculated relative changes in J_{sc} and V_{oc} of a high-efficiency solar cell due to the dissociation of Fe_iB_s pairs.[9]

III. BORON-OXYGEN-RELATED DEGRADATION

Degradation can also be observed in solar cells made on high-purity monocrystalline Cz–Si without any metal contamination. Although this effect was first observed more than three decades ago,[2] it was only recently found that it is related to the B_s and O_i concentrations in the Cz–Si material.[3,4] The experimental results suggested that a boron-oxygen complex is formed during illumination or minority-carrier injection in the dark.[3,10] The interstitial boron-interstitial oxygen (B_iO_i) pair, which had been detected before by deep-level transient capacitance spectroscopy (DLTS), was excluded as a possible candidate.[10] Apart from the fact that interstitial boron is not expected to exist in relevant concentrations in non-particle-irradiated silicon, the energy level of B_iO_i had been determined by DLTS to be at $E_C -0.26$ eV,[11] which is much shallower than the level of the light-induced boron-oxygen center.[10] As the latter center has evaded detection by DLTS so far, it has been studied extensively using injection- and temperature-dependent lifetime spectroscopy.[10,12] The energy level could be determined very accurately to be at $E_C -0.4$ eV,[12] clearly excluding the B_iO_i pair. The ratio of the electron to hole capture cross section was moreover found to be large ($\sigma_n/\sigma_p = 10$), suggesting a donorlike character of the center.[10]

Defect formation and annihilation have both been found to be thermally activated processes, but with strongly differing activation energies. For the defect formation process, a relatively low activation energy of $E_{gen} = 0.37$ eV has been determined by measuring the defect generation rate per center as a function of temperature in solar cells and lifetime samples.[13] For the defect annihilation process, an activation energy of $E_{ann} = 1.3$ eV was measured.[14] Furthermore, it was found that the defect generation rate is proportional to N_{dop}^2 and to the illumination intensity up to just 10^{-2} suns, above which it saturates.[15]

To elucidate the microscopic nature of the boron-oxygen complex, we have recently analyzed the dependence of the defect concentration on the boron and oxygen content quantitatively using a very large number of different Cz–Si materials.[15] As the center could not be detected by DLTS so far, we have applied the QSSPC method, enabling the accurate measurement of carrier recombination lifetimes as a function of injection level. Figure 3 shows the normalized defect concentration N_t^*, determined by subtracting the inverse lifetimes after and before light soaking, $N_t^* \equiv 1/\tau_d - 1/\tau_0$, as a function of the substitutional boron concentration $[B_s]$ for Cz–Si wafers with similar levels of oxygen contamination $[O_i] = (7-8) \times 10^{17}$ cm^{-3}. All lifetimes have been measured at a fixed injection level of $\eta = \Delta n/N_{dop} = 0.1$. As can be seen from Fig. 3, N_t^* increases proportionally with $[B_s]$.
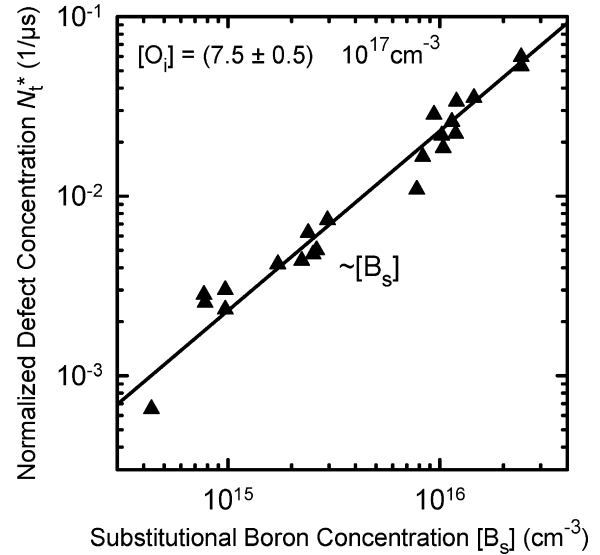

FIG. 3. Normalized defect concentration N_t^* as a function of the substitutional boron concentration $[B_s]$.[15]

As the same dependence was measured in several independent studies,[4,10,15] the proportionality between N_t^* and $[B_s]$ can be regarded as well established. Due to the relatively large scatter in the data, it had previously been very difficult to determined the exact quantitative dependence of the center's density on the interstitial oxygen concentration. Figure 4 shows the measured N_t^* values divided by the corresponding boron doping concentration N_{dop} as a function of the interstitial oxygen concentration $[O_i]$, which was determined from the 1107 cm^{-1} infrared absorption band. Plotting N_t^*/N_{dop} instead of N_t^* makes it possible to include Cz–Si wafers of different doping concentrations, extending the data base considerably. The most important result of Fig. 4 is
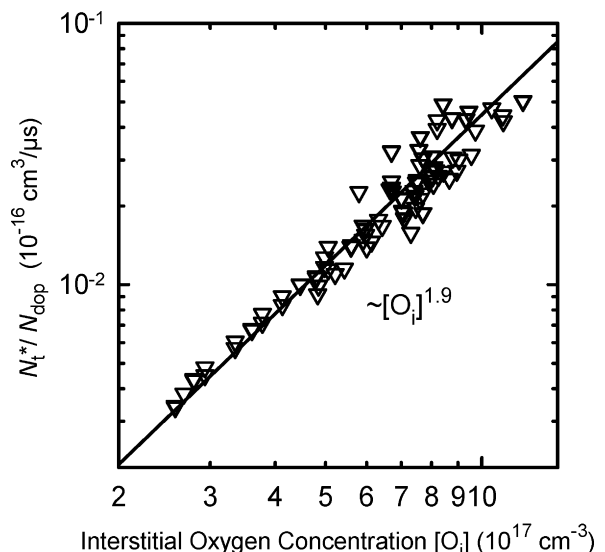

FIG. 4. Normalized defect concentration N_t^* as a function of the interstitial oxygen concentration $[B_s]$.[15]

the quadratic increase of N_t^* with $[O_i]$. This dependence could only recently be verified in an independent study.[16]

Based on the measured linear $N_t^*([B_s])$ and quadratic $N_t^*([O_i])$ dependencies, Schmidt et al.[15,17] have proposed a defect model involving interstitial oxygen dimers (O_{2i}). In this model, the presence of minority-carriers enhances the diffusivity of the oxygen dimers. The fast-diffusing O_{2i} is then trapped by B_s and forms a B_sO_{2i} complex, acting as a highly effective recombination center. The oxygen dimers are formed during the cooling of the silicon crystal after its growth or during the subsequent thermal donor annihilation treatment. The oxygen di-interstitial O_{2i} has been detected before in Cz–Si by infrared absorption, and a quadratic dependence of the O_{2i} equilibrium concentration on $[O_i]$ was found.[18] According to the proposed B_sO_{2i} model, this would lead to a quadratic dependence on the oxygen content for the concentration of the light-induced recombination center, in good agreement with the experimental results.

As known from theoretical calculations,[19] the stable form of the neutral oxygen dimer has a staggered configuration. Hence, a staggered configuration has also been proposed for the B_sO_{2i} complex as a possible core structure.[15] Interestingly, very recent density-functional calculations[20] have shown that the two most stable configurations of B_sO_{2i} are a square form, $B_sO_{2i}^{sq}$ [see Fig. 5(a)], and a staggered form, $B_sO_{2i}^{st}$ [see Fig. 5(b)], the latter one being equivalent to the structure proposed before.[15] The calculations also showed that $B_sO_{2i}^{sq}$ is the more stable configuration in the single positive charge state, while $B_sO_{2i}^{st}$ is the more stable when neutral.[20] The ionization energies of the B_sO_{2i} defect were calculated using the Marker Method.[20] These calculations revealed that $B_sO_{2i}^{sq}$ has in fact a (0/+) donor level in the upper half of the silicon band gap approximately between E_C −0.1 eV and E_C −0.3 eV, if the structure is confined to this geometry as is predicted for temperatures around room temperature, suggesting that $B_sO_{2i}^{sq+}$ is the most

likely candidate for the center responsible for the solar cell degradation.

While there is no disagreement in the literature that neutral O_{2i} has no energy level in the silicon band gap, very different values of the migration energy have been reported. While Ewels[19] calculated a migration energy of ~1.3 eV, making the dimer virtually immobile at room temperature, Lee et al.[21] have calculated a much lower migration barrier between 0.3 and 0.9 eV. Adey et al.[20] proposed recently that a positively charged oxygen dimer could be the fast-diffusing species in the defect reaction. Theoretical calculations have shown that the migration of a doubly positively charged oxygen dimer in a square configuration, O_{2i}^{sq++}, would result in a migration barrier of ~0.3 eV,[20] in good agreement with the experimental value of 0.37 eV measured for the activation energy of the defect formation.[13] Figure 6 shows how the migration of O_{2i}^{sq++} might proceed via a Bourgoin–Corbett mechanism:[20] (i) O_{2i}^{sq++} at position A in the silicon lattice traps an electron and becomes O_{2i}^{sq+}, (ii) O_{2i}^{sq+} transforms into the staggered configuration O_{2i}^{st+} with a barrier of just 0.2 eV, (iii) emission of an electron changes the charge state into O_{2i}^{st++}, (iv) the defect has to overcome a barrier of just 0.3 eV to move to another square configuration at position B. The binding energy E_B of O_{2i}^{++} to B_s^- has been determined by moving O_{2i}^{sq++} away from B_s^- by one and two steps, respectively, along the ⟨110⟩ direction in a large 144-atom supercell.[20] This increases the total energy by 0.38 eV in both cases, a value which can hence be identified with E_B. Furthermore, the migration energy E_m of O_{2i}^{sq++} has been calculated to be 0.86 eV (see Fig. 6). This results in an activation energy of $E_B + E_m = 1.24$ eV for the dissociation of the boron-oxygen complex, in excellent

(a)   **(b)**
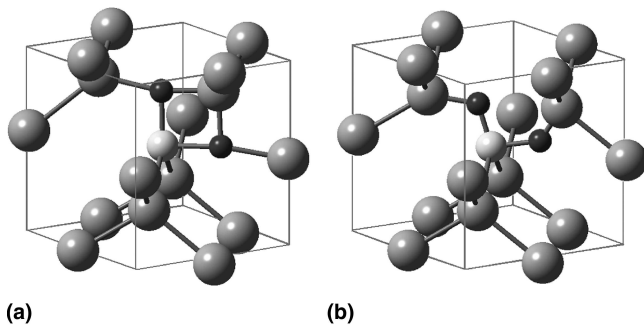
FIG. 5. Core structure of the two most stable configurations of B_sO_{2i} according to density-functional calculations.[20] (a) The square form $B_sO_{2i}^{sq}$ is the most stable form in the single positive charge state, while (b) the staggered configuration $B_sO_{2i}^{st}$ is more stable when its neutral (Si: grey balls, O_i: black balls, B_s: white balls).

FIG. 6. Configuration-coordinate diagram for the oxygen dimer. The arrows indicate the Bourgoin–Corbett diffusion mechanism proposed in Ref. 20.

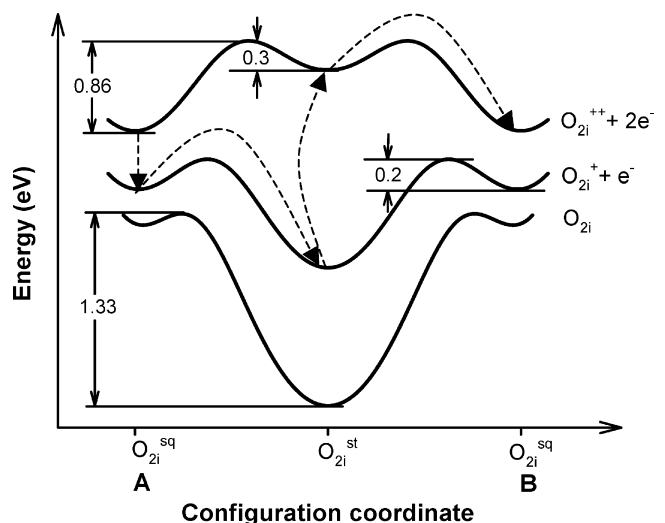agreement with the measured value of $E_{ann} = 1.3$ eV. It is interesting to note that it was shown that the double charge state of the oxygen dimer implies that the defect generation rate should be proportional to N_{dop}^2,[20] as indeed observed experimentally.[14]

IV. STRATEGIES FOR REDUCING THE BORON-OXYGEN DEGRADATION

A. Alternative Cz–Si materials

The direct correlation of the magnitude of degradation with the boron and the oxygen concentration in a Cz–Si wafer has been proved by means of carrier lifetime measurements on a very large number of Cz–Si wafers from different manufacturers.[3,4,15] Furthermore, measurements on Ga-doped p-type Cz–Si as well as on P-doped n-type Cz material have shown no degradation.[3,15] Based on these experimental results, several methods for reducing the lifetime degradation in Cz silicon solar cells have been proposed.[3] The two most promising approaches proposed in Ref. 3 were (i) replacement of B by another dopant, such as Ga or P (using p^+n solar cells in the latter case) and (ii) reduction of the oxygen concentration in the Cz material. Figure 7 shows the typical behavior of the different materials: while the carrier lifetime of conventional B-doped Cz–Si (solar-grade as well as electronic-grade material) degrades under illumination, Ga-doped Cz–Si of comparable doping concentration has a stable and much higher lifetime, comparable to that of B-doped FZ-Si, even if the interstitial oxygen concentration is approximately as high as in the case of the B-doped Cz material. The high oxygen concentration in silicon ingots grown with a conventional Cz single-crystal puller is due to the partial dissolution of the silica
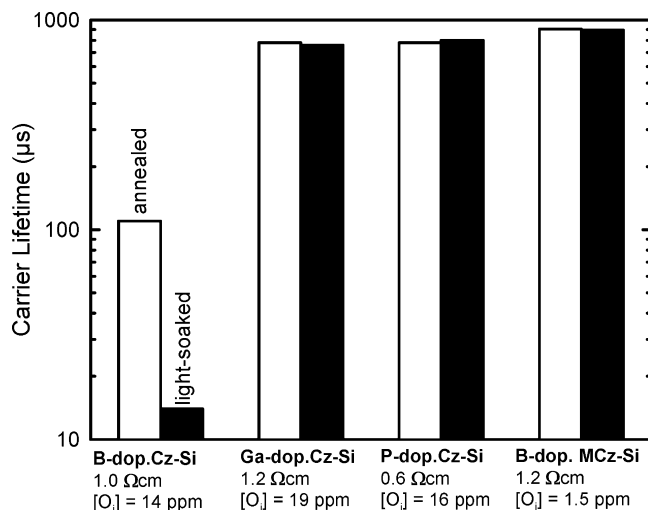
crucible during the growth process. The oxygen content can be strongly reduced by damping the melt flows with magnetic fields. This so-called magnetic-field assisted Cz (MCz) silicon with strongly reduced O_i concentration shows an almost vanishing light degradation (see Fig. 7) and has bulk lifetimes which are comparable to that of Ga-doped Cz–Si. Also included in Fig. 7 is a P-doped n-type Cz–Si material with high O_i content, which is also perfectly stable under illumination with white light.

High-efficiency solar cell processes were applied to the alternative Cz materials at different institutes and stable efficiencies well above 20% were obtained on Ga-doped Cz–Si, B-doped MCz material, and P-doped n-type Cz–Si (see Fig. 8).[22–26] For comparison, cell results obtained on B-doped FZ-Si and B-doped Cz–Si are also included in Fig. 8. Solar cell efficiencies above 20% can be achieved only with the alternative Cz materials, while the stable efficiency of cells fabricated on conventional 1 Ωcm B-doped Cz–Si is always well below 20%. Note that the degree of complexity of the three cell processes compared in Fig. 8 is very different, with the photolithography-based PERT (passivated emitter rear totally diffused cell) process being by far the most complex manufacturing process, whereas the obliquely evaporated contacts (OECO) process completely avoids any photolithography and alignment steps.

The segregation coefficient of Ga in Si is two orders of magnitude lower compared to that of B in Si. Thus, Ga-doped Cz–Si crystals exhibit a considerably higher variation in resistivity along their growth axis compared to B-doped crystals. Metz et al. have investigated the usability of a complete 6-in. Ga-doped Cz–Si crystal slab using the OECO solar cell process.[24] The resistivity of the crystal varied from 1.3 Ωcm at the top to 0.4 Ωcm in the tail region. Figure 9 shows the solar cell efficiencies, measured under standard testing conditions, as a function of the base resistivity. Peak efficiencies of up to

FIG. 7. Typical carrier lifetimes of of B-, Ga-, and P-doped Cz–Si and B-doped MCz–Si before and after light soaking. All lifetime measurement were performed using the microwave-detected photoconductance decay technique and a white bias light of 0.3 suns.
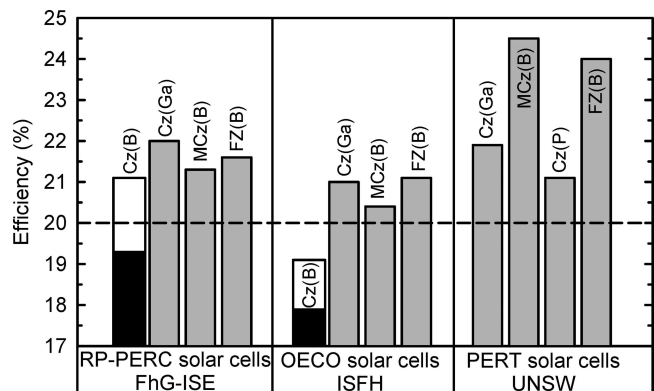
FIG. 8. Stable efficiencies of solar cells manufactured on alternative Cz–Si and FZ-Si (gray boxes). For comparison, cell efficiencies obtained on conventional B-doped Cz–Si before (white boxes) and after (black boxes) light degradation are shown (data taken from Refs. 22–26).
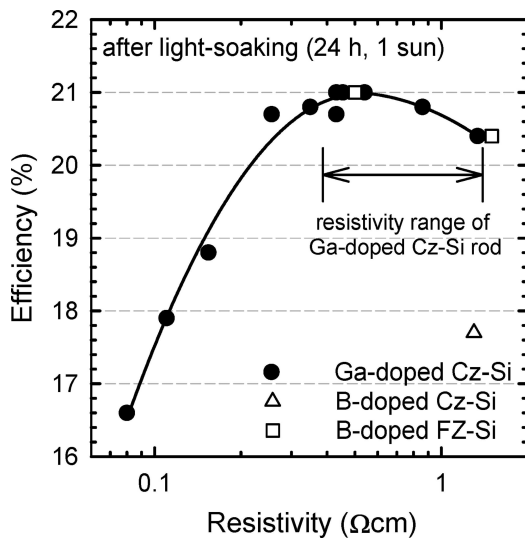
FIG. 9. Measured efficiencies of OECO solar cells manufactured on Ga-doped Cz–Si as a function of base resistivity (data taken from Ref. 24).

21% were obtained on 0.4 Ωcm material, and, more important, in the broad resistivity range between 0.25 and 1.34 Ωcm, cell efficiencies were found to reach more than 97% of the peak value, demonstrating that the inherent resistivity variations in Ga-doped Cz–Si crystals are well within the range tolerable for the manufacturing of high-efficiency solar cells.

B. Process optimization

Several approaches aiming at reducing the concentration of the metastable defect in B-doped Cz–Si during the solar cell manufacturing process have been investigated. In particular, certain high-temperature steps, optimized for Cz–Si, were found to be capable of significantly reducing the magnitude of degradation. In a recent comprehensive study, the high-temperature ($\sim$1050 °C) thermal oxidation process required for the growth of masking oxides and passivation layers was studied in detail.[4,27] It was found that the concentration of the metastable defect can be reduced by up to a factor of 4 if the ramping conditions are chosen properly. However, the absolute values of the stable lifetimes of conventional B-doped Cz–Si materials were still found to be on a relatively low level between about 20 and 45 μs after the optimized oxidation step, which is well below the lifetimes measured on Ga-doped Cz–Si and MCz materials. In a more recent study, a phosphorus emitter diffusion step at $\sim$850 °C with optimized ramping conditions was also found to have a beneficial effect on the magnitude of degradation, leading to a maximum reduction in the light-induced defect concentration by a factor of 3.5.[28] This effect was attributed to the temperature profile only and was shown to be not due to a gettering of impurities.[28] A permanent improvement of the carrier lifetime

in Cz–Si is possible not only using conventional quartz-tube furnaces. For example, a short annealing step of a few seconds at temperatures around 800 °C in a belt furnace was found to halve the light-induced defect concentration.[29] Similar results were obtained using rapid thermal processing.[30] It has also been conjectured that hydrogenation might reduce the degradation,[31] but definite experimental evidence is still lacking.

C. Adapted cell design

An alternative way to reduce the harmful effects of lifetime degradation on cell efficiency is to modify the cell design. By simply reducing the thickness of their solar cells to 100 μm, Münzer et al.[32] obtained a reduced degradation and an improved stable efficiency. However, this approach requires a very efficient rear surface passivation of the solar cell. Other solar cell structures, such as the emitter-wrap-through (EWT) cell,[33] also have the potential to reduce the light degradation considerably.

V. CONCLUSIONS

In this paper, we have discussed two different boron-related, electronically driven defect reactions, which are of particular importance for solar cells as they cause a severe degradation in the energy-conversion efficiency under illumination. If the silicon wafer is contaminated with iron, as is frequently the case for solar-grade multicrystalline silicon, iron-boron pairs form in equilibrium. Under illumination with white light, these pairs split up due to a recombination-enhanced dissociation reaction. As the recombination properties of iron-boron pairs and isolated iron are very different, the injection-dependent lifetime curves change considerably during light-soaking, and a characteristic crossover point exists. For injection levels below this characteristic crossover point the lifetime decreases during the dissociation of iron-boron pairs, while for injection levels above the crossover point it increases. On the basis of numerical device simulations, we have shown that the dissociation of iron-boron pairs always results in a degradation of the solar cell efficiency. However, the existence of the crossover point leads to a completely different behavior for the short-circuit current and the open-circuit voltage, as the two cell parameters are measured at very different excess-carrier concentrations. While the short-circuit current, measured at injection levels below the crossover point, always degrades during iron-boron dissociation, the open-circuit voltage may decrease, be constant, or even increase, depending on the excess-carrier concentration under open-circuit conditions relative to the position of the crossover point.

A pronounced degradation in solar cell efficiency under illumination can also be observed if high-purity

monocrystalline Czochralski-grown boron-doped silicon is used as the base material. This effect is attributed to the formation of a recombination-active boron-oxygen complex. The defect concentration depends linearly on the boron concentration and quadratically on the interstitial oxygen concentration, suggesting a defect complex made up of one substitutional boron and two interstitial oxygen atoms. Ab-initio calculations using density-functional theory show that such a type of defect exists in different stable configurations in crystalline silicon. In our defect formation model, a fast-diffusing oxygen dimer is captured by a substitutional boron atom. The diffusivity of the oxygen dimer is electronically enhanced via a Bourgoin–Corbett mechanism.

Various approaches to reduce or even completely avoid the boron-oxygen-related degradation exist. Alternative dopants, such as gallium or phosphorus, have been demonstrated to completely avoid the degradation. Reducing the oxygen content by applying a magnetic field during crystal growth is another way of improving the stable cell efficiency. In B-doped Cz–Si, high-temperature treatment can significantly reduce the magnitude of degradation. In combination with adapted cell structures, currently being developed in several labs, strongly improved stable efficiencies may also be expected in the near future on conventional B-doped Cz–Si.

ACKNOWLEDGMENTS

REFERENCES

1. D.H. Macdonald, L.J. Geerlings, and A. Azzizi: Iron detection in crystalline silicon by carrier lifetime measurements for arbitrary injection and doping. *J. Appl. Phys.* **95,** 1021 (2004).

2. H. Fischer and W. Pschunder: Investigation of photon and thermal induced changes in silicon solar cells. In *Proc. 10th IEEE Photovolt. Spec. Conf.* (IEEE, New York, 1973), p. 404.

3. J. Schmidt, A.G. Aberle, and R. Hezel: Investigation of carrier lifetime instabilities in Cz-grown silicon. In *Proc. 26th IEEE Photovolt. Spec. Conf.* (IEEE, New York, 1997), p. 13.

4. S.W. Glunz, S. Rein, W. Warta, J. Knobloch, and W. Wettling: On the degradation of Cz–Silicon solar cells, in *Proc. 2nd World Conf. Photovolt. Solar Energy Conv.* (EC, Ispra, Italy 1998), p. 1343.

5. K. Bothe, R. Hezel, and J. Schmidt: Recombination-enhanced formation of the metastable boron-oxygen complex in crystalline silicon. *Appl. Phys. Lett.* **83,** 1125 (2003).

6. A.A. Istratov, H. Hieslmair, and E.R. Weber: Iron and its complexes in silicon. *Appl. Phys. A* **69,** 13 (1999).

7. L.C. Kimerling and J.L. Benton: Electronically controlled reactions of interstitial iron in silicon. *Physica B* **116,** 297 (1983).

8. D. Macdonald and A. Cuevas: Reduced fill factors in multicrystalline silicon solar cells due to injection-level dependent bulk recombination lifetimes. *Prog. Photovolt.* **8,** 363 (2000).

9. J. Schmidt: Effect of dissociation of iron-boron pairs in crystalline silicon on solar cell properties. *Prog. Photovolt.* **13,** 325 (2005).

10. J. Schmidt and A. Cuevas: Electronic properties of light-induced recombination centers in boron-doped Czochralski silicon. *J. Appl. Phys.* **86,** 3175 (1999).

11. L.C. Kimerling, M.T. Asom, J.L. Benton, P.J. Drevinsky, and C.E. Caefer: Interstitial defect reactions in silicon. *Mater. Sci. Forum* **38–41,** 141 (1989).

12. S. Rein and S. Glunz: Electronic properties of the metastable defect in boron-doped Czochralski silicon: Unambiguous determination by advanced lifetime spectroscopy. *Appl. Phys. Lett.* **82,** 1054 (2003).

13. K. Bothe, R. Hezel, and J. Schmidt: Understanding and reducing the boron-oxygen-related performance degradation in Czochralski silicon solar cells. *Solid State Phenomena* **95–96,** 223 (2004).

14. S. Rein, T. Rehrl, W. Warta, S.W. Glunz, and G. Willeke: Electrical and thermal properties of the metastable defect in boron-doped Czochralski silicon, in *Proc. 17th European Photovolt. Solar Energy Conf.* (WIP-ETA, Munich, Germany, 2001), p. 1555.

15. J. Schmidt and K. Bothe: Structure and transformation of the metastable boron- and oxygen-related defect center in crystalline silicon. *Phys. Rev. B* **69,** 024107 (2004).

16. S. Rein, S.W. Glunz, and G. Willeke: Metastable defect in Cz–Si: Electrical properties and quantitative correlation with different impurities, in *Proc. 3rd World Conf. Photovolt. Solar Energy Conv.* (2003), p. 2899.

17. J. Schmidt, K. Bothe, and R. Hezel: Formation and annihilation of the metastable defect in boron-doped Czochralski silicon, in *Proc. 29th IEEE Photovolt. Spec. Conf.* (IEEE, New York, 2002), p. 178.

18. L.I. Murin, T. Hallberg, V.P. Markevich, and J.L. Lindström: Experimental evidence of the oxygen dimer in silicon. *Phys. Rev. Lett.* **80,** 93 (1998).

19. C.P. Ewels, Density functional modelling of point defects in semiconductors. Ph.D. Thesis, University of Exeter, U.K. (1997).

20. J. Adey, R. Jones, D.W. Palmer, P.R. Briddon, and S. Öberg: Degradation of boron-doped Czochralski silicon solar cells. *Phys. Rev. Lett.* **93,** 055504 (2004).

21. Y.J. Lee, J. von Boehm, M. Pesola, and R.M. Nieminen: Aggregation kinetics of thermal double donors in silicon. *Phys. Rev. Lett.* **86,** 3060 (2001).

22. S. Glunz, S. Rein, J. Knobloch, W. Wettling, and T. Abe: Comparison of boron- and gallium-doped *p*-type Czochralski silicon for photovoltaic application. *Prog. Photovolt.* **7,** 463 (1999).

23. S. Glunz, S. Rein, J. Lee, and W. Warta: Minority carrier lifetime degradation in boron-doped Czochralski silicon. *J. Appl. Phys.* **90,** 2397 (2001).

24. A. Metz, T. Abe, and R. Hezel: Gallium-doped Czochralski grown silicon: A novel promising material for the PV industry. *Proc. 16th European Photovolt. Solar Energy Conf.* (James & James, London, U.K., 2000), p. 1189.

25. J. Zhao, A. Wang, and M. Green: High efficiency PERT cells on a variety of single crystalline silicon substrates, in *Proc. 16th European Photovolt. Solar Energy Conf.* (James & James, London, U.K., 2000), p. 1100.

26. J. Zhao, A. Wang, and M. Green: Performance degradation in CZ(B) cells and improved stability high efficiency PERT and

PERL silicon cells on a variety of SEH MCZ(B), FZ(B) and CZ(Ga) substrates. *Prog. Photovolt.* **8,** 549 (2000).

27. S. Glunz, S. Rein, W. Warta, J. Knobloch, and W. Wettling: Degradation of carrier lifetime in Cz silicon solar cells. *Sol. Energy Mater. Sol. Cells* **65,** 219 (2001).

28. K. Bothe, J. Schmidt, and R. Hezel: Effective reduction of the metastable defect concentration in boron-doped Czochralski silicon for solar cells, in *Proc. 29th IEEE Photovolt. Spec. Conf.* (IEEE, New York, 2002), p. 194.

29. H. Nagel, A. Merkle, A. Metz, and R. Hezel: Permanent reduction of excess-carrier-induced recombination centers in solar grade Czochralski silicon by a short yet effective anneal, in *Proc. 16th European Photovolt. Solar Energy Conf.* (James & James, London, U.K., 2000), p. 1197.

30. J. Lee, S. Peters, S. Rein, and S. Glunz: Improvement of charge

minority-carrier lifetime in p(boron)-type Czochralski silicon by rapid thermal annealing. *Prog. Photovolt.* **9,** 417 (2001).

31. J. Schmidt and A. Cuevas: Progress in understanding and reducing the light degradation of Cz silicon solar cells, in *Proc. 16th European Photovolt. Solar Energy Conf.* (James & James, London, U.K., 2000) p. 1193.

32. K. Münzer, K. Holdermann, R. Schlosser, and S. Sterk: Thin monocrystalline silicon solar cells. *IEEE Trans. Electron Dev.* **46,** 2055 (1999).

33. S. Glunz, J. Dicker, J. Lee, R. Preu, S. Rein, E. Schneiderlöchner, J. Sölter, W. Warta, and G. Willeke: High-efficiency cell structures for medium-quality silicon, in *Proc. 17th European Photovolt. Solar Energy Conf.* (WIP-ETA, Munich, Germany, 2001), p. 1287.

12

J. Mater. Res., Vol. 21, No. 1, Jan 2006